LANDCOVER CLASSIFIACTION FOR FOREST MANAGEMENT USING ALOS-AVNIR-II IMAGES

Kyaw Sann OO, Masataka TAKAGI

Kochi University of Technology

ABSTRACT: AVNIR-II, PALSAR and PRISM sensors are assembled in Japanese earth observation satellite ALOS which orbiting the earth from outer space. Images from those sensors can apply in cartography, regional observation, disaster monitoring and resource surveying. Amount three sensors, AVNIR-II is a radiometer sensor with capabilities to acquire visible and near-infrared spectral range for observation of land and costal region of the earth from space. As the sensor provides images to generate landcover classification maps for monitoring regional environments, the landcover map is positively applicable in forest management with less cost. Since, there are many forests cover in remote area of Japan especially in Shikoku Island, they are require sustainable forest management in the reduction of greenhouse global warming by forest sinks. Once we have series of landcover datasets for all seasons, the forest classification could be done based on seasonal tree leaves changes and seasonal landuse changes. Normal Differential Vegetation Index calculation is an applicable technique to extract greenness of the tree leaves and it can analyze to class landcover for every year. Finally, proper forest management will be done by investigating year by year landcover changes using AVNIR-II satellite images.

KEYWORDS: forest management, landcover classification

1. INTRODUCTION

Kochi Prefecture is a mountainous remote area of Japan and it is located in the southern part of Shikoku Island. The prefecture gains 84% forest cover by large scale afforestation in the mid of 20th century. Once ages of the trees in this forest are fully developed for woods, the production is tremendous important with the fulfillment of multi-functions forest management in sustaining with carbon sinks. In particular, the forest carbon sinks can rewards removal of greenhouse gasses (especially CO_2) and production of oxygen by afforestation, reforestation and forest management. Consequently, forest management is the most important in greenhouse reduction in global warming consequence, since afforestation and reforestation are depending on limitation of land availability. In Japan, most of lands are covered with forests and only little land is available for afforestation or reforestation. Given that Japan set the target of removal of 13 Mt-C/year by forest, sustainable forest management is a major require action against global warming.

The advancement of satellite remote sensing is utilizing in frontier engineering applications, social sciences, natural resources management and many others. Every part of the earth surface can observe with satellite remote sensing. Based on availability of visible to near-infrared channels on optical remote sensing sensors, spectral reflectance of land surface features are acquiring from the space. Physical

remote sensors are converted the spectral reflectance of the earth surface objects to satellite image accumulating the spectral to several bands. A multispectral image generally includes 4 bands which are ranging from visible to near-infrared such as blue band, green band, red band and near-infrared band. Once we have red and near-infrared bands those bands are possible to calculate normalized differential vegetation index (NDVI).

Advance Visible and Near Infrared Radiometer type-2 (AVNIR-II) is one of ALOS satellite's sensors. AVNIR-II provides 10 meters spatial resolution image with 70 km swath width at nadir. One image has four multispectral bands and their wavelengths are listed in table 1.

Table 1-1: multispectral bands of AVNIR-II

Color	Band	Spectral region (micrometer)
Blue	1	0.42~0.50
Green	2	0.52~0.60
Red	3	0.61~0.69
Near-infrared	4	0.76~0.89

Bands' spectral regions are very useful to identify forest type. Concerning green leaves, they absorb solar radiation and appear relatively dark in the photosynthetically active radiation (PAR) spectral region while leaf cells reflect and transmit solar radiation and appear relatively bright in the near-infrared spectral region. Thus, NDVI is directly related to the photosynthetic capacity and hence energy absorption of plant canopies.

1.1 Problems

Proper sustainable forest management is needed based on three main following points.
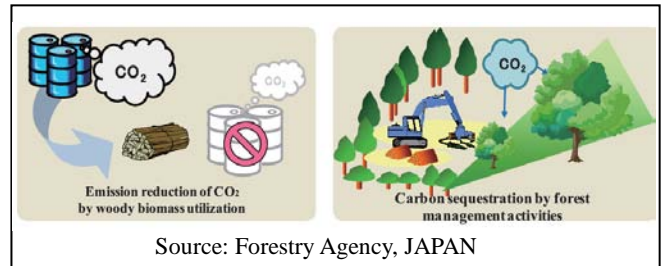

Source: Forestry Agency, JAPAN

Figure 1-1: Carbon sequestration by forest management activities

In Japan, afforestation of trees have been arriving at maturing stage for use as resources (*figure 1-1*) ; at the same time, the declination of forest workers is also becoming bigger by aging (*figure 1-2*). The aging rate is 26% in 2005. However, green employment project achieved recruitment of forest workers despite declination; mountainous areas are depopulating and aging due to the decline of public benefits of forests.
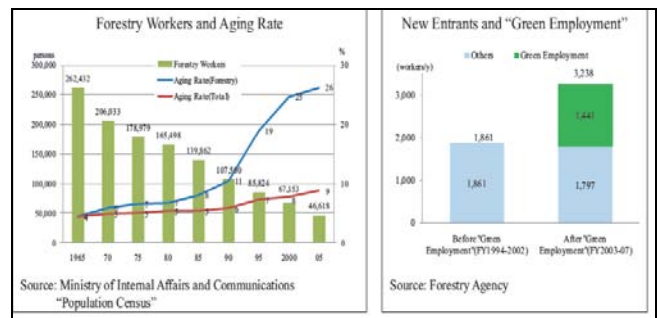

Figure 1-2: Forestry workers and aging rate

Forest carbon sinks (*figure 1-3*) is an important factors for action against global warming. Proper management on forest sector is requiring challenge toward the low carbon society.
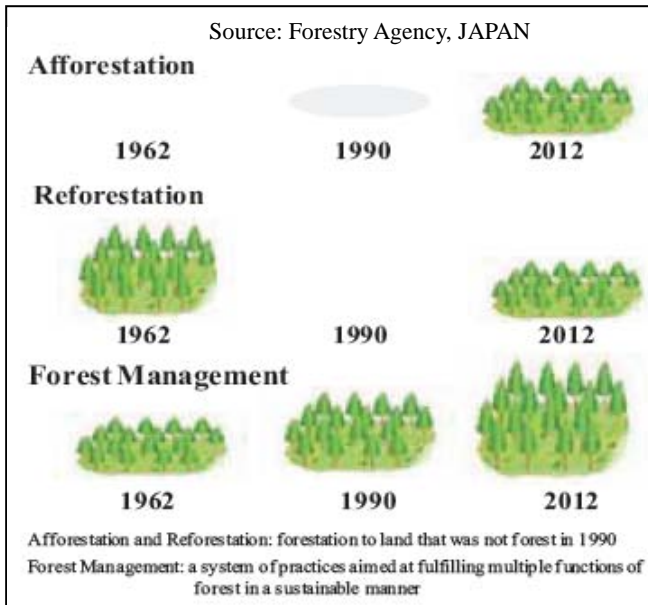
Figure 1-3: Forest carbon sinks

Finally, large-scale natural disasters in mountainous areas are becoming common due to frequent heavy rain or earthquakes (*figure 1-4*). Condition the forest areas are affected by large-scale disaster, the depending eco-system will be loosening the environmental equilibrium.
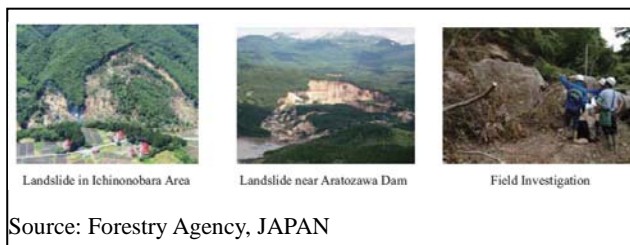

Figure 1-4: Large-scale disaster

1.2 Objectives

A major objective of the study is of sustainable forest management using satellite remote sensing to reduce greenhouse globe warming by forest carbon sinks (*figure 1-5*). Landcover maps will be generated from existing satellite images the forest management.
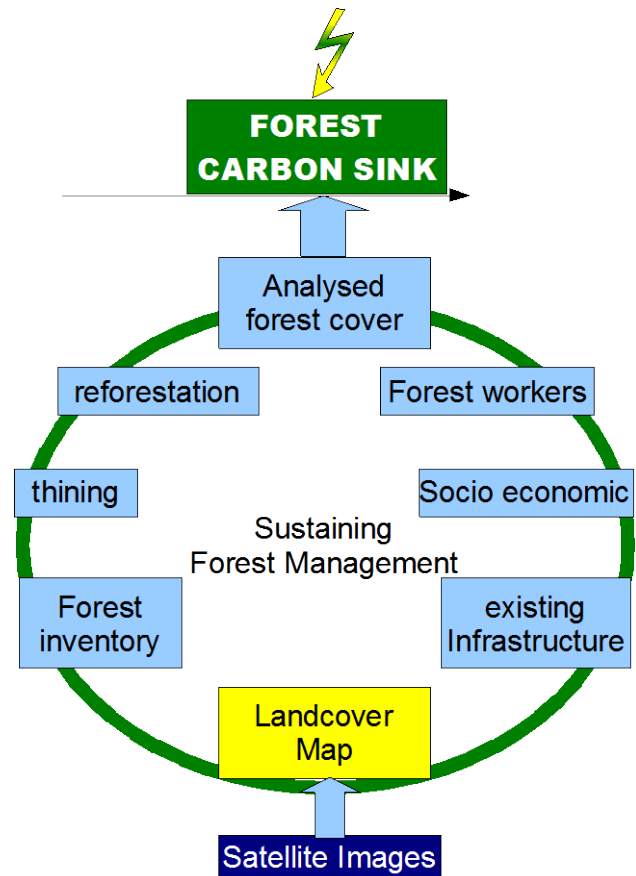

Figure 1-5: Satellite Remote Sensing for Green Cycle

Forest cover maps can use for proper forest management. Forest types can categorize from landcover. The landcover can classify using available satellite images.

Seasonal Normalized Differential Vegetation Index datasets can be calculated from red and near-infrared bands of multispectral image.

2. METHODOLOGY

Multispectral optical satellite images were used to generate forest cover map, as the matter the satellite sensors can detect wavelengths of vegetation reflectance. However, the image pixels are representing in digital number (DN) in satellite image; the DN numbers were converted to reflectance values using provided parameters. The main methodology of generation of forest cover

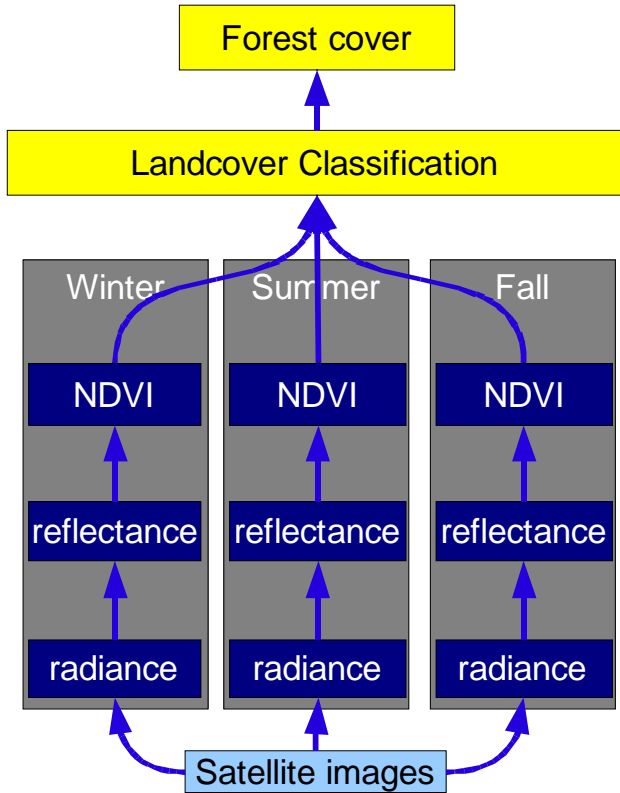from satellite image is presented in figure 2-1.

Figure 2-1: Generation of Forest cover

Two imageries of AVNIR-II were used in the study. Both of them were acquired in the same year in difference season (acquired on 2007-Feb-15 and 2007-Aug-18).

2.1 Background of NDVI calculation

The previous works were considered on the used of NOAA weather satellite. Advanced very high resolution radiometer (AVHRR) of NOAA satellite has detectors; two of which are sensitive to the wavelengths of light for vegetation ranging from 0.55~0.70 and 0.73~1.0 micrometers. These two channels were used to calculate NDVI. The classification of these NDVI values for vegetation classes are ~0.1 for barren areas, 0.2~0.3 for shrubs and grassland, 0.6~0.8 for temperate and tropical rainforest, respectively.

For the case of AVNIR-II, the classification of NDVI for vegetation classes can be used based on the similarity of band 3 and band 4 of AVNIR-II with wavelengths of AVHRR.

2.2 Radiance calculation

Radiance (L_λ) for spectral band λ at the sensor's aperture ($W/m^2/\mu m/sr$) can be calculated from digital number (*equation 1*).

$$L_\lambda = \frac{DN_\lambda}{Calcoef_\lambda \bullet Bandwidth_\lambda} \qquad (1)$$

where

$Calcoef_\lambda$ = Radiometric calibration coefficient (DN/ (mW/m^2-sr))

$Bandwith_\lambda$ = Bandwidth of spectral band λ (μm)

DN_λ = Digital Number of band λ

The above method isn't work unless radiometric calibration coefficient is provided. In this occasion another method (*equation 2*) can be applied using absolute calibration coefficients (gain and offset).

$$L_\lambda = Grescale * QCAL + Brescale \qquad (2)$$

where

L_λ = spectral radiance at the sensor's aperture in Watts/(m^2*ster*μm)

$QCAL$ = the quantized calibrated pixel value in DN

$Grescale$ = Rescaled gain (the data product "gain" contained in the Level 1 product header or ancillary data record) in watts/(meter squared * ster * μm)/DN

$Brescale$ = Rescaled bias (the data product "offset" contained in the Level 1 product header or ancillary data record) in watts/(meter squared * ster * μm)

The provided absolute calibration coefficients are listed in table 2 for each band of images.

Table 2-1: Absolute calibration coefficients

Band	2007-Feb-15 (gain, offset)	2007-Aug-18 (gain, offset)
1	0.588, 0.0	0.588, 0.0
2	0.573, 0.0	0.573, 0.0
3	0.502, 0.0	0.502, 0.0
4	0.557, 0.0	0.835, 0.0

The above table (*table 2-1*) shows only in band 4 (near infrared channel) has difference in absolute calibration coefficient in two seasons.

2.3 Reflectance calculation

Reflectance images were calculated to reduce the image-to-image illumination differences by normalizing from solar irradiance. Band dependant planetary reflectance is defined as:

$$\rho_p = \frac{\pi \bullet L_\lambda \bullet d^2}{ESUN_\lambda \bullet \cos\theta_s} \text{ or } \rho_p = \frac{\pi \bullet L_\lambda}{(F_0 \bullet \cos\theta_s / d^2)} \quad (3)$$

where

ρ_p = Unitless planetary reflectance

L_λ = radiance for spectral band λ at the sensor's aperture (W/m^2/μm/sr)

d = Earth-Sun distance in astronomical units

F_0 *or* $ESUN_\lambda$ = Mean solar exoatmospheric irradiance (W/m^2/μm)

θ_λ = Solar zenith angle

Mean solar exoatmospheric irradiance (ESUN$_\lambda$) was acquired from the table of Hiroshi Murakami and et al. (2007) (*table 2-3*).

Table 2-2: Mean solar exoatmospheric irradiance for AVNIR-II

Band	λc[nm]	F$_0$[W/m^2/μm]
1	463.0	1943.3
2	560.0	1813.7
3	652.1	1562.3
4	820.6	1076.5

In consequent, coefficients were generated for all bands of each image (*table 2.3*).

Table 2-3: Absolute calibration coefficients

$\pi/[F_0 cos\theta/d2]$	2007-Feb-15	2007-Aug-18
Band 1	0.0017626	0.00185324
Band 2	0.0018886	0.00198567
Band 3	0.0021925	0.00230519
Band 4	0.0031819	0.00334547

2.4 Normalized Differential Vegetation Index (NDVI)

Normalized Difference Vegetation Index is the most common measurement of vegetation classification. Satellite images are used to calculate NDVI using red band and near-infrared band of multispectral (*equation 4*).

$$NDVI = \frac{NIR - VIS}{NIR + VIS} \quad (4)$$

where

NDVI = Normalized Difference Vegetation Index

NIR = Spectral reflectance of near infrared region

VIS = Spectral reflectance of visible region (red)

NDVI values will range from -1 to +1 with vegetated areas are in greater than 0. The range of data values can maximize to unsigned integer.

$$scaleNDVI = 100(NDVI + 1) \quad (5)$$

where

NDVI = Normalized Difference Vegetation Index

scaleNDVI = maximized range of NDVI to unsigned integer

Calculated NDVI images were presented in the result section of the paper (*figure 4-1 & 4-2*).

3. CLASSIFICATION

The greenness values of forest cover could be monitored from differences of annual forest cover. A classification for land cover map was done after the

NDVI values were scaled (*equation 5*) using below decision tree (*table 3-1*).

Table 3-1: Logic of classification

Logic (A=Feb, B=Aug)	Feature
$A \leq 82 \cap B \leq 89$	Water
$82 \leq A \leq 105 \cap 89 \leq B \leq 104$	Barren
$105 \leq A \leq 107$ (skip B, cloud)	Vegetation
$107 \leq A \leq 125$ (skip B, cloud)	Grass
$146 \leq A \leq 164 \cap 145 \leq B \leq 161$	Bamboo
$164 \leq A \leq 168 \cap 161 \leq B \leq 167$	Evergreen
$125 \leq A \leq 146 \cap 171 \leq B$	Deciduous

The classification of land-cover classes using above logic were presented in the figure 3-1. NDVI Values were selected virtually from known features in the classification.
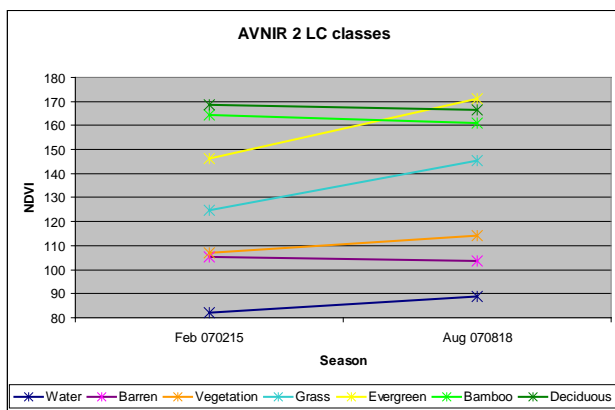

Figure 3-1: AVNIR-II classes

4. RESULT

A landcover (*figure 4-3*) was classified from calculated NDVI values. Generated NDVI for each season were presented in figure 4-1 and 4-2.

Table 4-1: Statistic of landcover classes

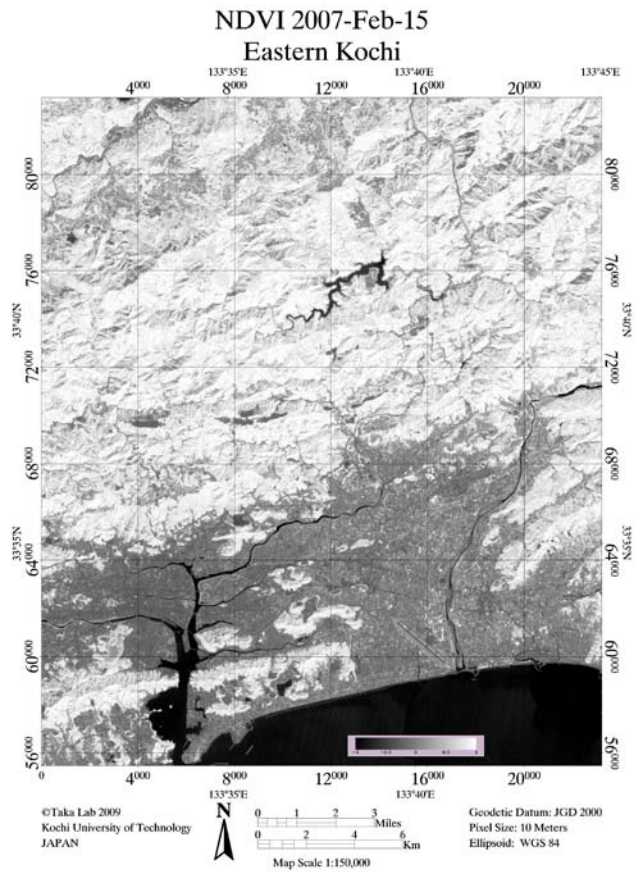| Classes	Sq. KM	Percentage
Water	62.0959	9.7 %
Barren	36.6211	5.7 %
Vegetation	10.6849	1.7 %
Grasses	110.5191	17.2 %
Deciduous	11.2254	1.7 %
Evergreen	301.4955	46.9 %
Bamboo	110.8291	17.2 %

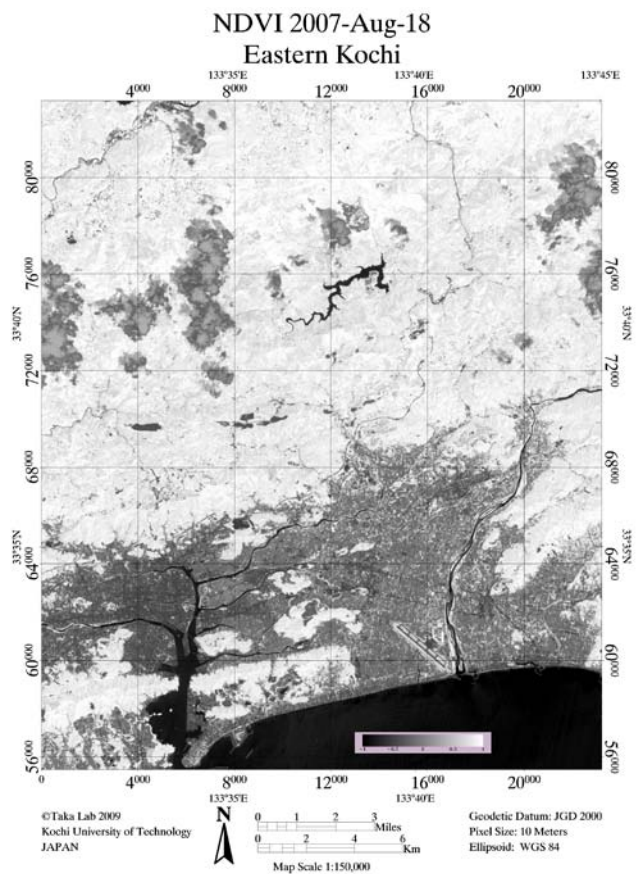Figure 4-1: NVDI map for 2007-Feb-15

Figure 4-2: NVDI map for 2007-Aug-18

The result (*table 4-1*) presented that the evergreen forest is the most populated forest cover in the selected area and it is already maturing for woody biomass production. In this occasion, proper management of forest is very important to keep carbon offsets continuously and forest sinks equilibrium.
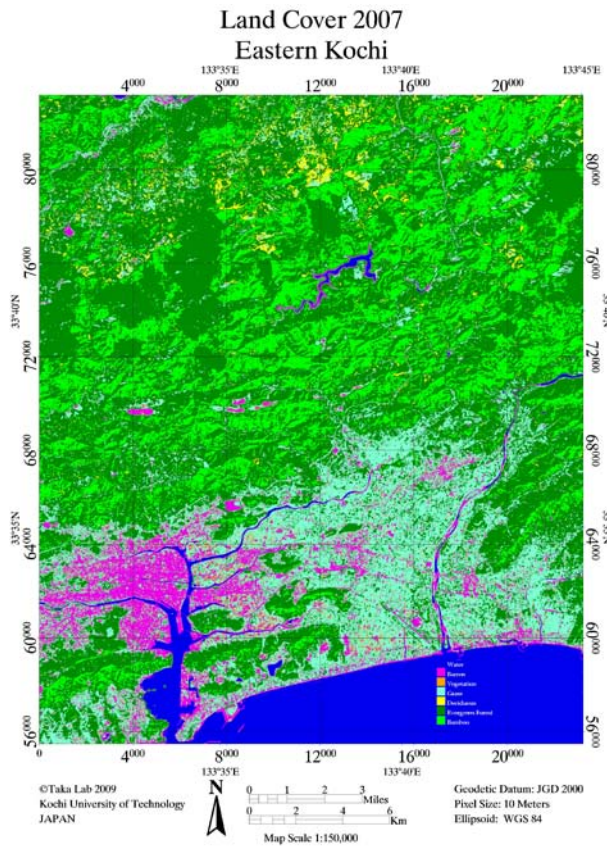

Figure 4-3: 2007 landcover map

5. DISCUSSION

The greenness values of forest cover could be monitored from differences of annual forest cover. Though, a period of greenness value was represented by calculating NDVI from satellite image in this study, more satellite datasets will require in forest cover changes detection phenomena.

An approach is presented for forest management (*figure 5-1*). It can be a possible way to use landcover map in the sustainable forest management, afforestation, reforestation from the

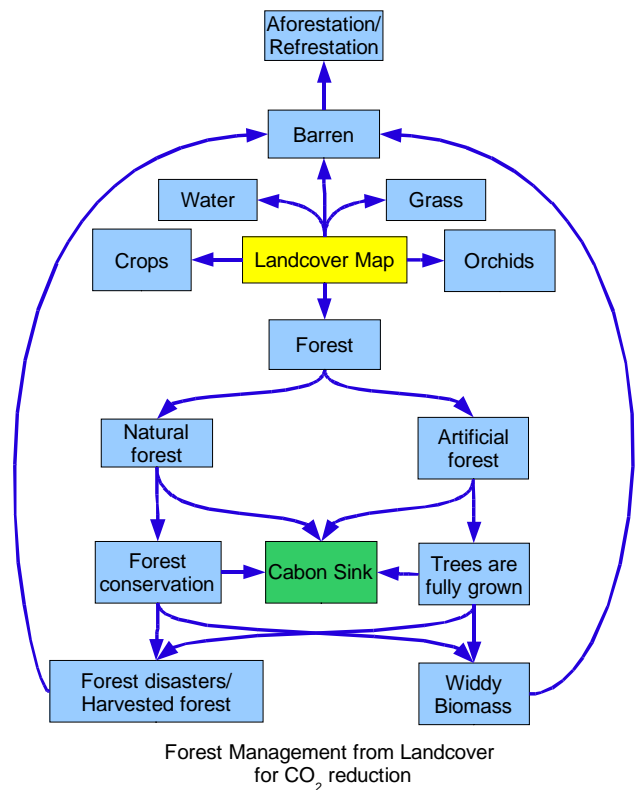point of reduction of greenhouse global warming by forest carbon sinks.

Figure 5-1: Possible philosophy for reduction of global warming

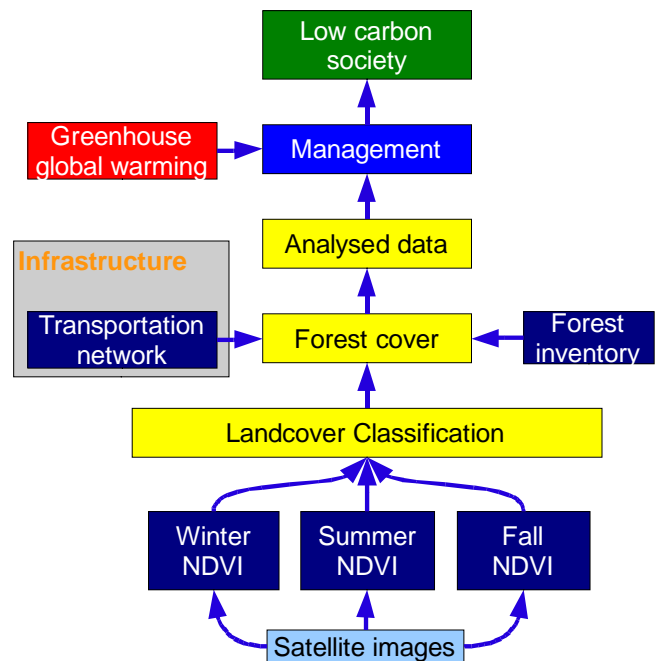Moreover, there is a proposal presented to go to the low carbon society (*figure 5-2*).

Figure 5-2: Toward low carbon society

REFERENCES

AVNIR-2, 2006. *About ALOS*, Japanese Aerospace Exploration Agency's website information, URL: http://www.eorc.jaxa.jp/ALOS/en/about/avnir2.htm, JAXA (last date accessed: 15 Dec 2009).

Eidenshink, J.C. and Faundeen, J.L., 1994. The 1km AVHRR global land data set: first stage in implementation, *International Journal of Remote Sensing*, 15 (17): 3443-3462, 1994

Forest Agency, 2008. *Annual Report on Trends in Forest and Forestry FY2008*, Fiscal Year 2008 Summary Report, URL: http://www.maff.go.jp/e/index.html. The Ministry of Agriculture, Forestry and Fisheries of JAPAN (last date accessed: 15 Dec 2009).

Gates, David M., 1980. *Biophysical Ecology*, Springer-Verlag, New York, 611 p.

Hiroshi Murakami, et al., 2007. Brightness mutual proofreading of AVNIR-2 and MODIS that uses directionality function of the atmospheric top reflectivity, ALOS special issue, *Journal of the Japan Society of Photogrammetry and Remote Sensing*, Vol. 27, No. 4, 2007 p. 354-362.

John Weier and David Herring, 2000. Measuring Vegetation (NDVI & EVI), internet information, URL:http://earthobservatory.nasa.gov/Features/MeasuringVegetation/, NASA (last date accessed: 15 Dec 2009).

Kageyama Koji and Wahid Din Ara, 2007. ALOS/AVNIR-2 satellite image's phonologic???, JSPRS, Vol. 46, No. 4, 2007, p. 16-19.

Landcover Classification Project, Center for Earth Observation. Internet Information, URL: http://www.yale.edu/ceo/Projects/swap/landcover/, Yale University, USA, (last date accessed: 15 Dec 2009).

Landsat 7 Science Data User's Handbook, internet information, URL: http://landsathandbook.gsfc.nasa.gov/handbook/handbook_htmls/chapter11/chapter11.html, NASA (last date accessed: 15 Dec 2009).

Rouse, J. W., R. H. Haas, J. A. Schell, and D. W. Deering, 1973. Monitoring vegetation systems in the Great Plains with ERTS, *Third ERTS Symposium*, NASA SP-351 I, 309-317.

Myneni, R. B., F. G. Hall, P.J. Sellers, and A.L. Marshak, 1995. The interpretation of spectral vegetation indexes, *IEEE Transactions on Geoscience and Remote Sensing*, 33, 481-486.

Sellers, P. J., 1985. Canopy reflectance, photosynthesis, and transpiration, *International Journal of Remote Sensing*, 6, 1335-1372.

Smith, Ronald B.; Foster, Jane; Gleason, Arthur C.; Kouchoukos, Nicholas; Gluhosky, Paul; dePauw, Eddy, 1997. A climate and vegetation atlas of the fertile crescent, The Yale Center of Earth Observation, Yale University

Yuta Inoue and Tsunemi Watanabe, 2008. *Feasibility analysis of acquiring forest certification system in the Monobe River basin's forest*, SSMS2008 Symposium paper, URL: http://management.kochi-tech.ac.jp/PDF/COEReport_2008/2.4/05%20YutaInoue-watanabe%20tsunemi.pdf, Society for Social Management Systems - Infrastructure and Environment, 6-8 March 2008, Kochi, JAPAN (last date accessed: 15 Dec 2009).